

# Systemic Induction of Photosynthesis via Illumination of the Shoot Apex Is Mediated Sequentially by Phytochrome B, Auxin and Hydrogen Peroxide in Tomato<sup>1</sup>[OPEN]

Zhixin Guo, Feng Wang, Xun Xiang, Golam Jalal Ahammed, Mengmeng Wang, Eugen Onac, Jie Zhou, Xiaojian Xia, Kai Shi, Xueren Yin, Kunsong Chen, Jingquan Yu, Christine H. Foyer, and Yanhong Zhou\*

Department of Horticulture, Zijingang Campus, Zhejiang University, Hangzhou 310058, People's Republic of China (Z.G., F.W., Xu.X., G.J.A., J.Z., Xi.X., K.S., X.Y., K.C., J.Y., Y.Z.); Philips Research Europe, High Tech Campus 34, 5656 AE Eindhoven, The Netherlands (M.W., E.O.); Zhejiang Provincial Key Laboratory of Horticultural Plant Integrative Biology, Hangzhou 310058, People's Republic of China (K.C., J.Y., Y.Z.); and Centre for Plant Sciences, Faculty of Biology, University of Leeds, Leeds LS2 9JT, United Kingdom (C.H.F.)

ORCID IDs: 0000-0001-5351-1531 (F.W.); 0000-0001-9943-9977 (Xu.X.); 0000-0001-7292-9802 (E.O.); 0000-0001-5989-6989 (C.H.F.).

Systemic signaling of upper leaves promotes the induction of photosynthesis in lower leaves, allowing more efficient use of light flecks. However, the nature of the systemic signals has remained elusive. Here, we show that preillumination of the tomato (*Solanum lycopersicum*) shoot apex alone can accelerate photosynthetic induction in distal leaves and that this process is light quality dependent, where red light promotes and far-red light delays photosynthetic induction. Grafting the wild-type rootstock with a *phytochrome B* (*phyB*) mutant scion compromised light-induced photosynthetic induction as well as auxin biosynthesis in the shoot apex, auxin signaling, and *RESPIRATORY BURST OXIDASE HOMOLOG1* (*RBOH1*)-dependent hydrogen peroxide ( $H_2O_2$ ) production in the systemic leaves. Light-induced systemic  $H_2O_2$  production in the leaves of the rootstock also was absent in plants grafted with an auxin-resistant *diageotropica* (*dgt*) mutant scion. Cyclic electron flow around photosystem I and associated ATP production were increased in the systemic leaves by exposure of the apex to red light. This enhancement was compromised in the systemic leaves of the wild-type rootstock with *phyB* and *dgt* mutant scions and also in *RBOH1*-RNA interference leaves with the wild type as scion. Silencing of *ORANGE RIPENING*, which encodes NAD(P)H dehydrogenase, compromised the systemic induction of photosynthesis. Taken together, these results demonstrate that exposure to red light triggers *phyB*-mediated auxin synthesis in the apex, leading to  $H_2O_2$  generation in systemic leaves. Enhanced  $H_2O_2$  levels in turn activate cyclic electron flow and ATP production, leading to a faster induction of photosynthetic  $CO_2$  assimilation in the systemic leaves, allowing plants better adaptation to the changing light environment.

As a consequence of their sessile lifestyle, plants have evolved a high capacity for the regulation of physiology, growth, and development that facilitates survival in a constantly changing environment. Environmental stimuli perceived within an organ not only influence morphogenetic and physiological changes within that

organ but also generate systemic effects in other organs that are remote from the site of signal perception. This crucial phenomenon is called systemic signaling or systemic regulation. Systemic signaling prepares other tissues of a plant for future challenges that may initially only be sensed by a few local tissues or cells. Several types of systemic responses are known. These include systemic acquired resistance, which is typically activated by pathogens such as viruses, bacteria, and fungi (Fu and Dong, 2013), induced systemic resistance, which is triggered by beneficial soil microorganisms or others (Pieterse and Dicke, 2007), and systemic acquired acclimation, which is initiated by abiotic stresses such as high light, UV radiation, heat, cold, and salinity (Mittler and Blumwald, 2015).

The light utilization efficiency of photosynthesis is important for the survival of understory plants and plants growing in canopies. In particular, the efficient use of the energy contained in light (sun) flecks is important because light flecks contribute up to 60% to 80% of photosynthetically active radiation received by understory plants (Percy and Seemann, 1990; Leakey et al., 2003, 2005). Earlier studies have shown the existence of systemic regulation of stomatal development

<sup>1</sup> This work was supported by the National Natural Science Foundation of China (grant nos. 31672198 and 31430076), the Special Fund for Agro-Scientific Research in the Public Interest (grant no. 201203004), the Fundamental Research Funds for the Central Universities (grant no. 2016XZZX001-07), the National High Technology R&D Program of China (grant no. 2013AA102406), and the Fok Ying-Tong Education Foundation (grant no. 132024).

\* Address correspondence to [yanhongzhou@zju.edu.cn](mailto:yanhongzhou@zju.edu.cn).

The author responsible for distribution of materials integral to the findings presented in this article in accordance with the policy described in the Instructions for Authors ([www.plantphysiol.org](http://www.plantphysiol.org)) is: Yanhong Zhou ([yanhongzhou@zju.edu.cn](mailto:yanhongzhou@zju.edu.cn)).

Y.Z. and J.Y. designed the research; Z.G., F.W., and Xu.X. performed the research; all authors analyzed the data; G.A., M.W., E.O., J.Z., Xi.X., K.S., X.Y., and K.C. discussed the data; Y.Z., J.Y., and C.H.F. wrote the article with contributions from the other authors.

[OPEN] Articles can be viewed without a subscription.

[www.plantphysiol.org/cgi/doi/10.1104/pp.16.01202](http://www.plantphysiol.org/cgi/doi/10.1104/pp.16.01202)

and of photosynthesis in developing leaves in response to environmental signals perceived by mature leaves, such as changing irradiance and atmospheric CO<sub>2</sub> conditions (Lake et al., 2002; Coupe et al., 2006; Araya et al., 2008). Phytochrome B (phyB) is important in the transmission of the systemic signals that modulate stomatal development in young leaves of *Arabidopsis thaliana*; Casson and Hetherington, 2014). In tomato (*Solanum lycopersicum*), there are two forms of phyB, phyB1 and phyB2, that work together to mediate red (R) light-induced responses, such as hypocotyl elongation and greening in seedlings (Hauser et al., 1995; Weller et al., 2000).

Photosynthesis is completely switched off in the dark, specifically to prevent futile cycling of metabolites through the reductive and oxidative pentose phosphate pathways. Hence, leaves need time to reactivate the enzymes of carbon assimilation after a period of darkness. The time taken to reach maximum net rates of photosynthesis upon illumination is called photosynthetic induction (Walker, 1973). Systemic signaling also has been observed for the regulation of photosynthesis in relation to leaf ontology in understory plants (Montgomery and Givnish, 2008). The uppermost leaves, which are generally the first to receive sunlight, display faster photosynthetic induction times than understory leaves (Bai et al., 2008). Photosynthetic induction in understory leaves is enhanced by the preillumination of upper leaves but not lower leaves, suggesting a directional signal transfer (Hou et al., 2015). While this process allows plants to use the light energy in sun flecks more efficiently, the nature of the systemic signals and their transmission pathways remain largely unresolved. Although systemic signaling between different leaf ranks has been suggested to occur through the xylem (Thorpe et al., 2007) and also via electrical signals (Zimmermann et al., 2009), it is likely that systemic signals also pass through the phloem (Turgeon and Wolf, 2009; Hou et al., 2015). In addition, the phytohormone auxin is produced in the shoot apex and redistributed throughout the shoot by rapid nonpolar phloem transport (Ljung et al., 2001). Changes in the light environment can dramatically alter auxin homeostasis, which is regulated in a light quality- and photoreceptor-dependent manner (Halliday et al., 2009).

The photosynthetic electron transport chain exhibits enormous flexibility in the relative rates of NADPH and ATP production in order to accommodate the varying requirements of metabolism (Foyer et al., 2012). Non-cyclic, pseudocyclic, and cyclic electron flow (CEF) pathways operate in the photosynthetic electron transport chain to drive the proton gradient across the thylakoid membrane (Allen, 2003). Photosynthetic induction is not only associated with the activation of the light- and thiol-dependent activation of carbon assimilation enzymes but also dependent on a high rate of CEF to drive ATP synthesis (Foyer et al., 1992). Considerable overreduction of the electron transport acceptors occurs during the photosynthetic induction period, and this continues until carbon assimilation can

be activated. CEF around PSI, an essential component of photosynthesis, drives the proton gradient in a situation when NADP reduction has reached its highest capacity and this essential electron acceptor is no longer available (Yamori et al., 2015; Yamori and Shikanai, 2016). CEF is particularly sensitive to the reduction-oxidation (redox) status of the chloroplast, which in turn is responsive to cellular redox homeostasis. Oxidants such as hydrogen peroxide (H<sub>2</sub>O<sub>2</sub>), which are produced by pseudocyclic electron flow in the chloroplasts, play a crucial role in the activation of CEF through modulation of the activity of the NADPH-plastoquinone reductase complex (Strand et al., 2015). Hormone-mediated generation of H<sub>2</sub>O<sub>2</sub> also can stimulate CO<sub>2</sub> assimilation (Jiang et al., 2012).

Auxins such as indole-3-acetic acid (IAA) generate H<sub>2</sub>O<sub>2</sub> (Ivanchenko et al., 2013; Peer et al., 2013) and can regulate CO<sub>2</sub> assimilation (Bidwell and Turner, 1966; Hayat et al., 2009; Peng et al., 2013). Therefore, we used tomato plants to test the hypothesis that the systemic signaling that regulates photosynthetic induction in understory leaves arises from light-induced changes in auxin and H<sub>2</sub>O<sub>2</sub> homeostasis involving the modulation of CEF in systemic leaves. We present evidence showing that R light perceived in the shoot apex by a phyB-dependent pathway alters IAA signaling in a systemic manner. IAA signals from the apex, perceived in distal leaves, trigger systemic H<sub>2</sub>O<sub>2</sub> production that accelerates photosynthetic induction by increasing CEF-dependent ATP production in the systemic leaves. These findings provide new insights into the elaborate plant regulatory network that allows light adaptation in different organs.

## RESULTS

### Systemic Induction of Photosynthesis in the Distal Leaves of Tomato Plants Is Dependent on PhyB in the Shoot Apex

To examine the role of light perception by the remote organs in the induction of photosynthesis in distal leaves, either the uppermost fully expanded leaves (fifth and sixth leaves), the first to third leaves on the stem, or the shoot apex were exposed to white light (WL) at an intensity of 300  $\mu\text{mol m}^{-2} \text{s}^{-1}$  for 30 min, while other leaves were left in the dark (Supplemental Fig. S1). The induction of CO<sub>2</sub> assimilation upon exposure to high light (1,500  $\mu\text{mol m}^{-2} \text{s}^{-1}$  photosynthetic photon flux density [PPFD]) was then followed in the fourth leaves on the stem for 30 min. A preillumination of either the upper expanded leaves or the lower leaves did not significantly change the times required to reach 50% (T50) and 90% (T90) of the maximal CO<sub>2</sub> assimilation rates in the fourth leaves (systemic leaf; Fig. 1B). In contrast, exposure of the apex to WL for 30 min resulted in a faster induction of CO<sub>2</sub> assimilation in the fourth leaves as compared with the dark controls. The T50 and T90 were decreased from 8.17 to 4.30 min and from 19.7 to 14.7 min, respectively (Fig. 1, A and B). However, such an induction of photosynthesis was observed only when the PPFD was higher than the light

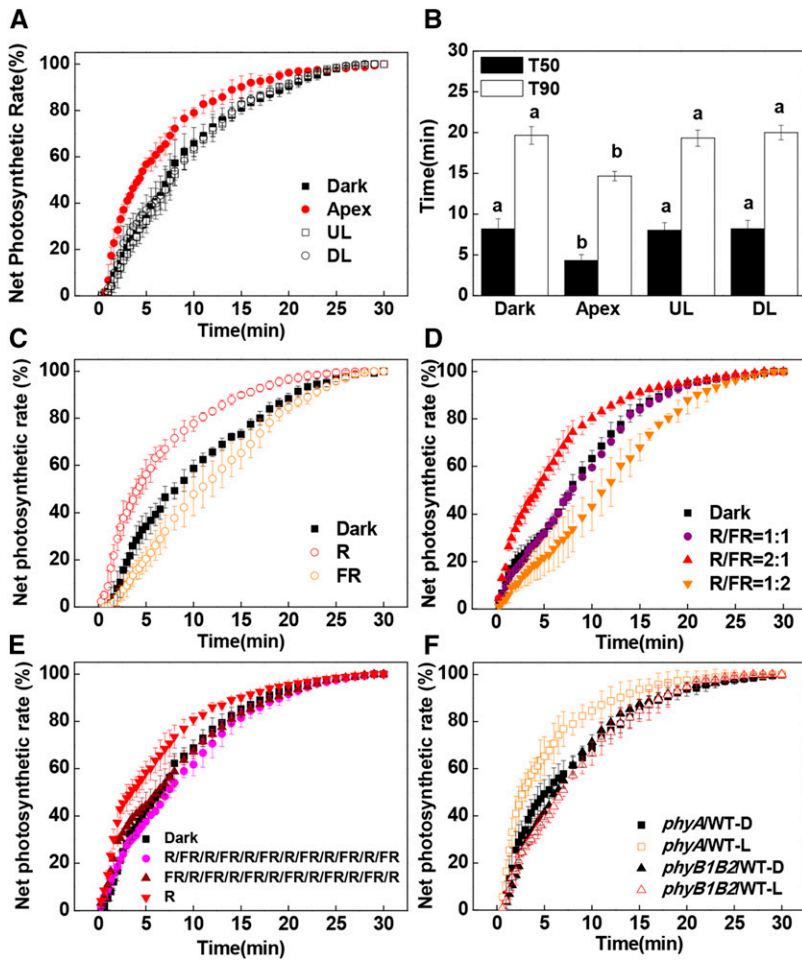


**Figure 1.** Influence of systemic light signaling on the induction phase of net CO<sub>2</sub> assimilation (A and C–F) and T50 or T90 (B). A and B, Preillumination was provided to the shoot apex, upper leaves (UL; fifth and sixth leaves), and lower leaves (LL; first to third leaves) with WL at an intensity of 300  $\mu\text{mol m}^{-2} \text{s}^{-1}$  for 30 min before CO<sub>2</sub> assimilation was analyzed in the fourth leaves. C, The apex was preilluminated with R or FR light for 30 min before CO<sub>2</sub> assimilation was analyzed in the fourth leaves. D, The apex was preilluminated with different R/FR light ratios for 30 min, in which R light was kept at 300  $\mu\text{mol m}^{-2} \text{s}^{-1}$ , before CO<sub>2</sub> assimilation was measured in the fourth leaves. E, A reciprocal R/FR light pulse at 5-min intervals with six cycles was applied on the apex before CO<sub>2</sub> assimilation was measured in the fourth leaves. F, Preillumination was provided by WL at an intensity of 300  $\mu\text{mol m}^{-2} \text{s}^{-1}$  for 30 min before CO<sub>2</sub> assimilation was analyzed in the fourth leaves of the grafted plants. During the illumination treatments, the other parts of the plant were kept in darkness. Net photosynthetic rates are expressed as percentage of the maximum net CO<sub>2</sub> assimilation. Plants without preillumination (dark [D]) were used as controls. L, WL. Values are means of four plants  $\pm$  sd. Different letters indicate significant differences at  $P < 0.05$  according to Tukey's test.

compensation point (approximately 50  $\mu\text{mol m}^{-2} \text{s}^{-1}$ ; Supplemental Fig. S2). These findings demonstrate that only the light perceived by the shoot apex was able to transmit systemic signals to the systemic leaves in order to facilitate a more rapid induction of CO<sub>2</sub> assimilation.

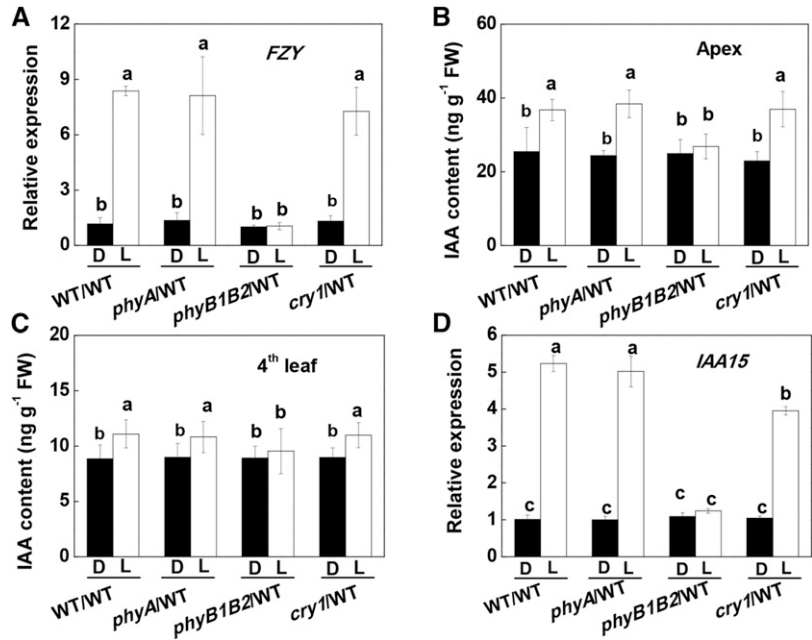
To determine the nature of the signals that facilitate a more rapid induction of CO<sub>2</sub> assimilation in the systemic leaves, we applied red (R; 660 nm) and far-red (FR; 735 nm) light at an intensity of 300  $\mu\text{mol m}^{-2} \text{s}^{-1}$  to the shoot apex for 30 min prior to the measurement of the induction of CO<sub>2</sub> assimilation in the distal (fourth) leaves (Supplemental Fig. S1). R light enhanced photosynthetic induction, while FR light delayed the induction of CO<sub>2</sub> assimilation in the fourth leaves (Fig. 1C). Interestingly, R light-induced photosynthesis was abolished when R light was supplemented with FR light at red/far-red (R/FR) light ratios of 1:1 and 1:2, but the stimulation of photosynthetic induction was still observed at an R/FR light ratio of 2:1 (Fig. 1D). Moreover, reciprocal R/FR light exposures at 5-min intervals for up to six cycles failed to enhance the rate of photosynthetic induction (Fig. 1E). We then grafted the young shoots of wild-type tomatoes and tomato mutants deficient in phyA (*phyA*), phytochrome B1 and B2 (*phyB1B2*), or cryptochrome 1 (*cry1*) with two developing leaves onto stems of wild-type plants with

four leaves. This resulted in four grafting combinations: WT/WT, *phyA*/WT, *phyB1B2*/WT, and *cry1*/WT. As had been observed in the wild-type plants, a preillumination with WL for 30 min resulted in a faster induction of CO<sub>2</sub> assimilation in the rootstock leaves (fourth leaf) of the WT/WT, *phyA*/WT, and *cry1*/WT plants compared with dark controls (Fig. 1F; Supplemental Figs. S3 and S4). In contrast, the WL-dependent induction of CO<sub>2</sub> assimilation was compromised in *phyB1B2*/WT plants, which showed little change in the T50 and T90 values compared with the leaves of the wild-type plants (Fig. 1F; Supplemental Fig. S4). However, chlorophyll content in the developing leaves of *phyB1B2* was not significantly different from that in wild-type plants (data not shown). This finding demonstrates that phyB signaling in the apex plays a critical role in the enhancement of photosynthetic induction in distal systemic leaves.

#### PhyB-Mediated Auxin Signaling Is Required for the Systemic Enhancement of Photosynthetic Induction

Photoreceptors modify plant growth, development, and stress responses via alterations in phytohormone homeostasis (Jiao et al., 2007; Wang et al., 2016). Like polar auxin transport (PAT), light-induced signaling is

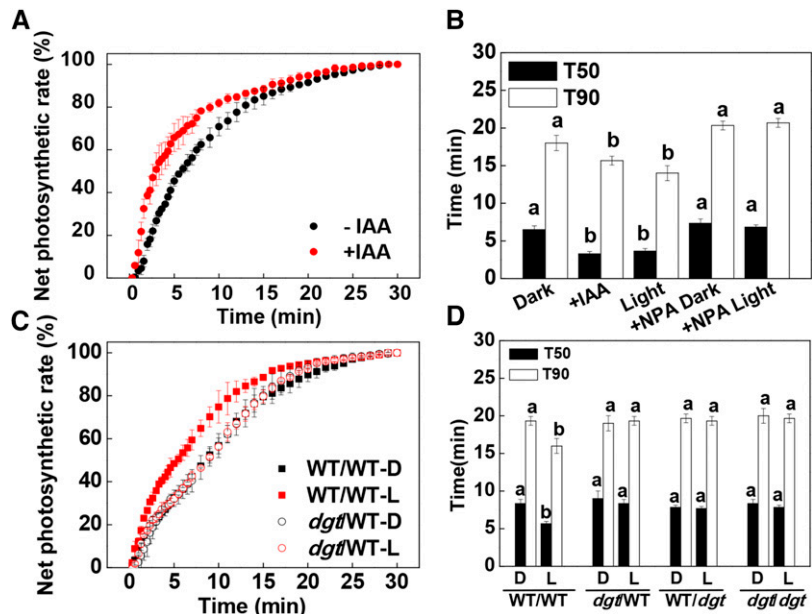
**Figure 2.** Effects of preillumination of the apex on *FZY* and *IAA15* transcript levels and on the accumulation of IAA in grafted plants. A, *FZY* transcript levels in the apex. B, IAA accumulation in the apex. C and D, IAA accumulation (C) and *IAA15* transcript levels (D) in the fourth leaves. Samples were harvested at 30 min after the preillumination. Plants without preillumination (dark [D]) were used as controls. L, WL. During the illumination treatments, the other parts of the plant were kept in darkness. Values are means of four plants  $\pm$  SD. Different letters indicate significant differences at  $P < 0.05$  according to Tukey's test. FW, Fresh weight.



basipetal in direction. Therefore, we examined how auxin accumulation was modified in the WT/WT, *phyA*/WT, *phyB1B2*/WT, and *cry1*/WT lines before and after the apex of the plants was exposed to WL. A preillumination with WL induced transcript levels of *FLAVIN MONOOXYGENASE* (*FZY*) in the apex and the accumulation of IAA in the apex and the fourth leaves (Fig. 2, A–C). *FZY* encodes *FZY*, a critical enzyme involved in a rate-limiting step of IAA biosynthesis (Tivendale et al., 2010). Similar increases also were found in the apex and the fourth leaves of the *phyA*/WT and *cry1*/WT plants. In contrast, WL failed

to increase *FZY* transcripts or IAA accumulation in either the apex or the fourth leaves of the *phyB1B2*/WT plants. Similar to increased IAA accumulation, WL induced an accumulation of *IAA15* transcripts, a marker of IAA signaling (Deng et al., 2012), and *PIN1* transcripts, a marker for PAT (Geldner et al., 2001; Ivanchenko et al., 2015), by 3- to 5-fold in the systemic leaves of the WT/WT, *phyA*/WT, and *cry1*/WT plants but not in the rootstock leaves of the *phyB1B2*/WT plants (Fig. 2D; Supplemental Fig. S5). Taken together, these results indicate that *phyB* was responsible not only for the observed increases in IAA biosynthesis in

**Figure 3.** Rate of net CO<sub>2</sub> assimilation (A and C) during the induction phase of photosynthesis in fourth leaves and T50 or T90 (B and D). A and B, Effects of IAA (10  $\mu$ M) and NPA (10  $\mu$ M) on the induction phase of CO<sub>2</sub> assimilation in the fourth leaves and the time required to reach T50 or T90. C and D, Induction of CO<sub>2</sub> assimilation in the fourth leaves and T50 or T90 of the grafted plants with *dgt* as scion or rootstock. D, Dark control; L, WL (300  $\mu$ mol m<sup>-2</sup> s<sup>-1</sup>) applied to the apex for 30 min before the measurement of CO<sub>2</sub> assimilation and the harvest of samples. During the illumination treatments, the other parts of the plant were kept in darkness. Net photosynthesis rates are expressed as percentages of the maximum rate of net CO<sub>2</sub> assimilation. Values are means of four plants  $\pm$  SD. Different letters indicate significant differences at  $P < 0.05$  according to Tukey's test.



the apex but also for auxin signaling at the levels of the systemic leaves.

To explore the role of increased IAA accumulation on the systemic enhancement of photosynthetic induction, we applied IAA and *N*-1-naphthylphthalamic acid (NPA; an inhibitor for PAT) to the shoot apex either in the dark conditions or just prior to the preillumination treatment. Similar to the preillumination treatment, the application of IAA accelerated the induction of CO<sub>2</sub> assimilation in the systemic leaves. However, the application of NPA abolished the WL-induced enhancement of photosynthetic induction in the systemic leaves (Fig. 3, A and B; Supplemental Fig. S6). Therefore, we concluded that IAA synthesized in the apex may function as a systemic signal to influence the rate of induction of CO<sub>2</sub> assimilation in the distal leaves. To confirm this hypothesis, we grafted shoots with two leaves of wild-type and cyclophilin *A diageotropica* (*dgt*) mutant plants, which are auxin resistant, onto the stem at the fourth leaf position of either wild-type or *dgt* rootstock, respectively. In this way, we were able to examine how the induction of CO<sub>2</sub> assimilation in the

fourth leaf was altered by changes in the auxin signal arising in the apex. As predicted, WL preillumination-induced enhancement of the induction of CO<sub>2</sub> assimilation was abolished in the wild-type leaves of the *dgt*/WT plants and in the *dgt* leaves of WT/*dgt* plants. Moreover, the T50 and T90 values were not changed by the preillumination (Fig. 3, C and D; Supplemental Fig. S7A). Taken together, these results indicate that auxin signaling is essential for the preillumination-induced enhancement of the induction of CO<sub>2</sub> assimilation in systemic leaves.

#### Auxin-Triggered H<sub>2</sub>O<sub>2</sub> Accumulation Leads to Systemic Increases in the Induction of Photosynthesis by Activating CEF

Reactive oxygen species such as H<sub>2</sub>O<sub>2</sub>, which are produced in the apoplast, can function as secondary messengers in hormone signaling pathways that underpin plant development and stress responses (Xia et al., 2015). In these studies, preillumination of the apex triggered an accumulation of transcripts encoding

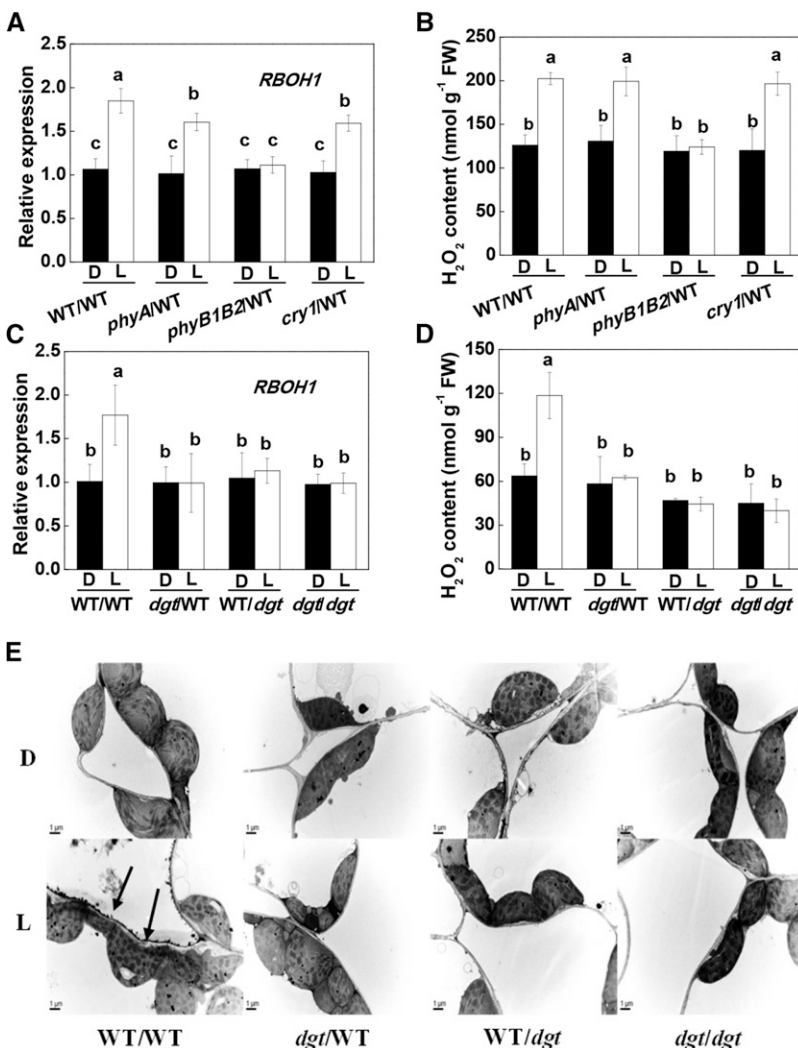


**Figure 4.** Influence of scion genotypes and lighting on the levels of *RBOH1* transcripts and H<sub>2</sub>O<sub>2</sub> accumulation in the systemic leaves. A, Influence of different photoreceptor mutants as scions on the levels of *RBOH1* transcripts in the systemic leaves of grafted plants. B, Influence of different photoreceptor mutants as scions on the accumulation of H<sub>2</sub>O<sub>2</sub> in the systemic leaves of grafted plants. C, *RBOH1* transcripts in the systemic leaves in plants with *dgt* as scion or rootstock. D, Accumulation of H<sub>2</sub>O<sub>2</sub> in the systemic leaves in grafted plants with *dgt* as scion or rootstock. E, Cytochemical localization of H<sub>2</sub>O<sub>2</sub> accumulation in mesophyll cells of systemic leaves with CeCl<sub>3</sub> staining in grafted plants with *dgt* as scion or rootstock. The apex was exposed to WL (L) at 300  $\mu\text{mol m}^{-2} \text{s}^{-1}$  for 30 min or not (dark [D]), then the fourth leaves (systemic leaf) of the grafted plants were harvested for the analysis and cytochemical detection of H<sub>2</sub>O<sub>2</sub>. During the illumination treatments, the other parts of the plant were kept in darkness. Values in A to D are means of four plants  $\pm$  SD, with different letters indicating significant differences at  $P < 0.05$  according to Tukey's test. Arrows in E indicate that H<sub>2</sub>O<sub>2</sub>-induced CeCl<sub>3</sub> precipitates in the apoplast of systemic leaves. FW, Fresh weight.

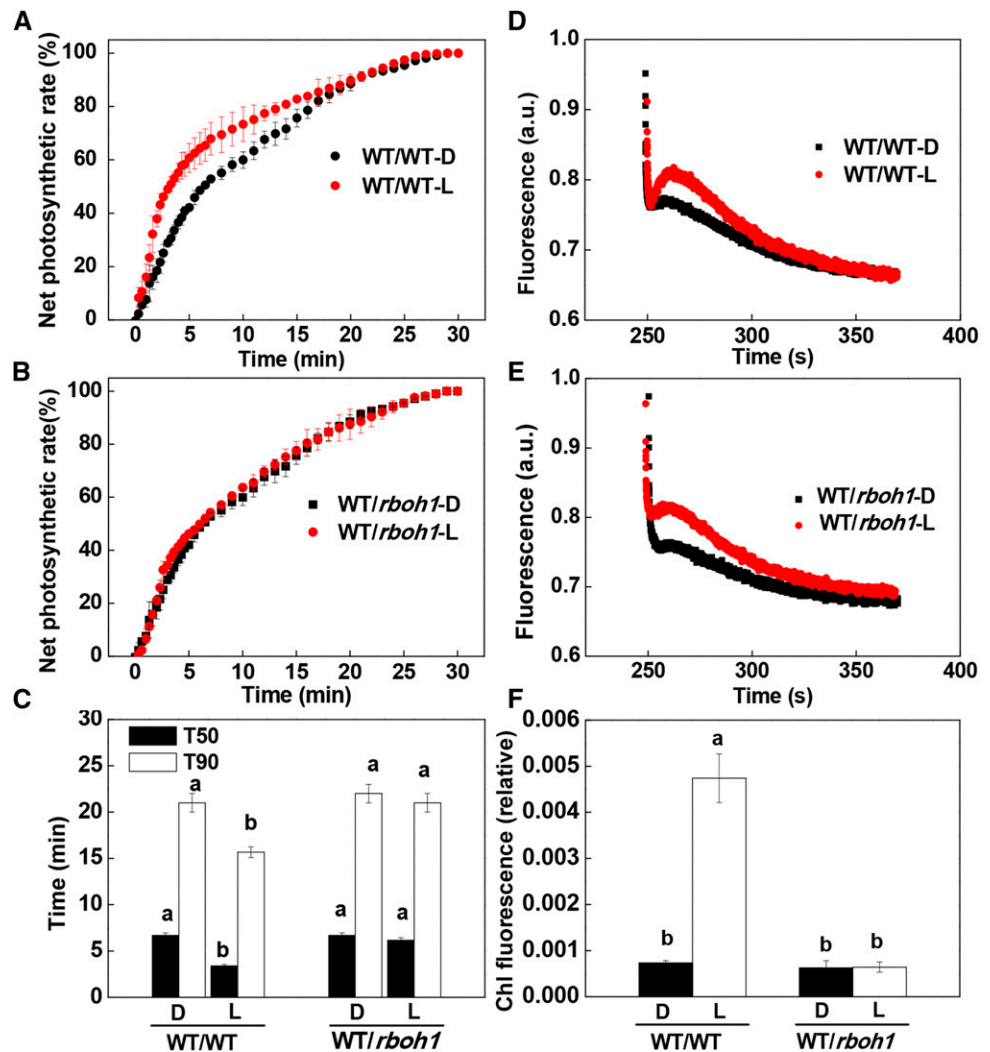
RESPIRATORY BURST OXIDASE HOMOLOG1 (*RBOH1*), together with an accumulation of  $H_2O_2$  in the systemic leaves of the WT/WT, *phyA*/WT, and *cry1*/WT plants but not in the rootstock leaves of the *phyB1B2*/WT plants (Fig. 4, A and B). Similarly,  $H_2O_2$  accumulation was observed in the walls of the mesophyll cells of the fourth leaf of WT/WT plants, particularly those facing the intercellular spaces, as indicated by the increased deposits of  $CeCl_3$  staining (Fig. 4E). However, the light-induced increases in *RBOH1* transcript levels and apoplastic  $H_2O_2$  accumulation were abolished in the systemic leaves of *dgt*/WT, WT/*dgt*, or *dgt*/*dgt* plants (Fig. 4, C–E). These results suggest that illumination of the apex resulted in apoplastic  $H_2O_2$  accumulation in the systemic leaves and that this process was dependent on auxin signaling.

To determine the role of *RBOH1* in the preillumination-dependent enhancement of photosynthetic induction in the systemic leaves, we generated *RBOH1*-RNA interference (RNAi) plants (*rboh1*) and grafted them to wild-type plants. The fourth leaves of the *rboh1* plants with the wild type as scion had approximately 50% of

the *RBOH1* transcripts compared with that in WT/WT leaves (Supplemental Fig. S8). Significantly, the preillumination-induced enhancement of photosynthetic induction was compromised in the systemic *rboh1* leaves of WT/*rboh1* and *rboh1*/*rboh1* plants (Fig. 5, A–C; Supplemental Fig. S9A). Taken together, these results indicate that auxin-induced  $H_2O_2$  production in the systemic leaves plays a critical role in the preillumination-associated enhancement of the induction of  $CO_2$  assimilation.

CEF around PSI is particularly important in the induction phase of photosynthesis because it generates ATP at a time when noncyclic electron flow is limited by the availability of NADP (Joët et al., 2002; Joliot and Joliot, 2002). We compared rates of CEF in the systemic leaves of the WT/WT, WT/*rboh1*, and *rboh1*/*rboh1* plants. The preillumination treatment of the apex significantly increased rates of CEF in the leaves of WT/WT plants. This increase was not observed in the systemic leaves of WT/*rboh1* or *rboh1*/*rboh1* plants (Fig. 5, D–F; Supplemental Fig. S9, B and C). No enhancement of the rates of CEF was observed in the

**Figure 5.** Requirement for *RBOH1* in systemic light signaling from the shoot apex to distal leaves for the regulation of  $CO_2$  assimilation rates and CEF during the induction phase of photosynthesis. A to C, Time course of increases in net photosynthesis rate during photosynthetic induction and T50 or T90 in the fourth leaves. Net photosynthetic rates are expressed as percentages of the maximum net photosynthesis rate. D and E, Typical traces of chlorophyll *a* fluorescence quenching after 4 min of actinic illumination ( $250 \mu\text{mol m}^{-2} \text{s}^{-1}$ ) in grafted plants with *rboh1* mutant rootstocks. a.u., Arbitrary unit. F, Relative chlorophyll (Chl) fluorescence expressed as the rate ratio of the induction curve. Irradiance to the shoot apex (top lighting) was performed with WL (L) at  $300 \mu\text{mol m}^{-2} \text{s}^{-1}$  for 30 min. Plants without preillumination (dark [D]) were used as controls. During the illumination treatments, the other parts of the plant were kept in darkness. Values are means of four plants  $\pm$  sd. Different letters indicate significant differences at  $P < 0.05$  according to Tukey's test.



systemic leaves of *phyB1B2*/WT plants, *dgt*/WT plants, WT/*dgt* plants, or *dgt/dgt* plants (Fig. 6; Supplemental Fig. S7B). However, increased CEF rates were observed in the systemic leaves of the *phyA*/WT and *cry1*/WT plants. These observations demonstrate that preillumination of the apex enhanced rates of CEF in an  $H_2O_2$ -dependent manner and that this was linked to the activity of the *RBOH1* NADPH oxidase in the systemic leaves.

CEF-dependent ATP production is particularly important during the induction phase of photosynthesis because it drives electron transport and associated  $CO_2$

assimilation when the electron acceptor NADP is in short supply (Foyer et al., 2012). An increase in the ATP content of 47.2% to 57.7% was observed in the systemic wild-type leaves of WT/WT, *phyA*/WT, and *cry1*/WT plants after the apex had been illuminated with WL for 30 min followed by exposure of the fourth leaves to WL for 8 min. The top lighting-induced increase in ATP production was not found in the wild-type leaves of the *phyB1B2*/WT and *dgt*/WT plants (Fig. 7, A and B). Furthermore, ATP levels were not increased in the *rboh1* leaves after the preillumination treatment in the WT/*rboh1* plants (Fig. 7C).

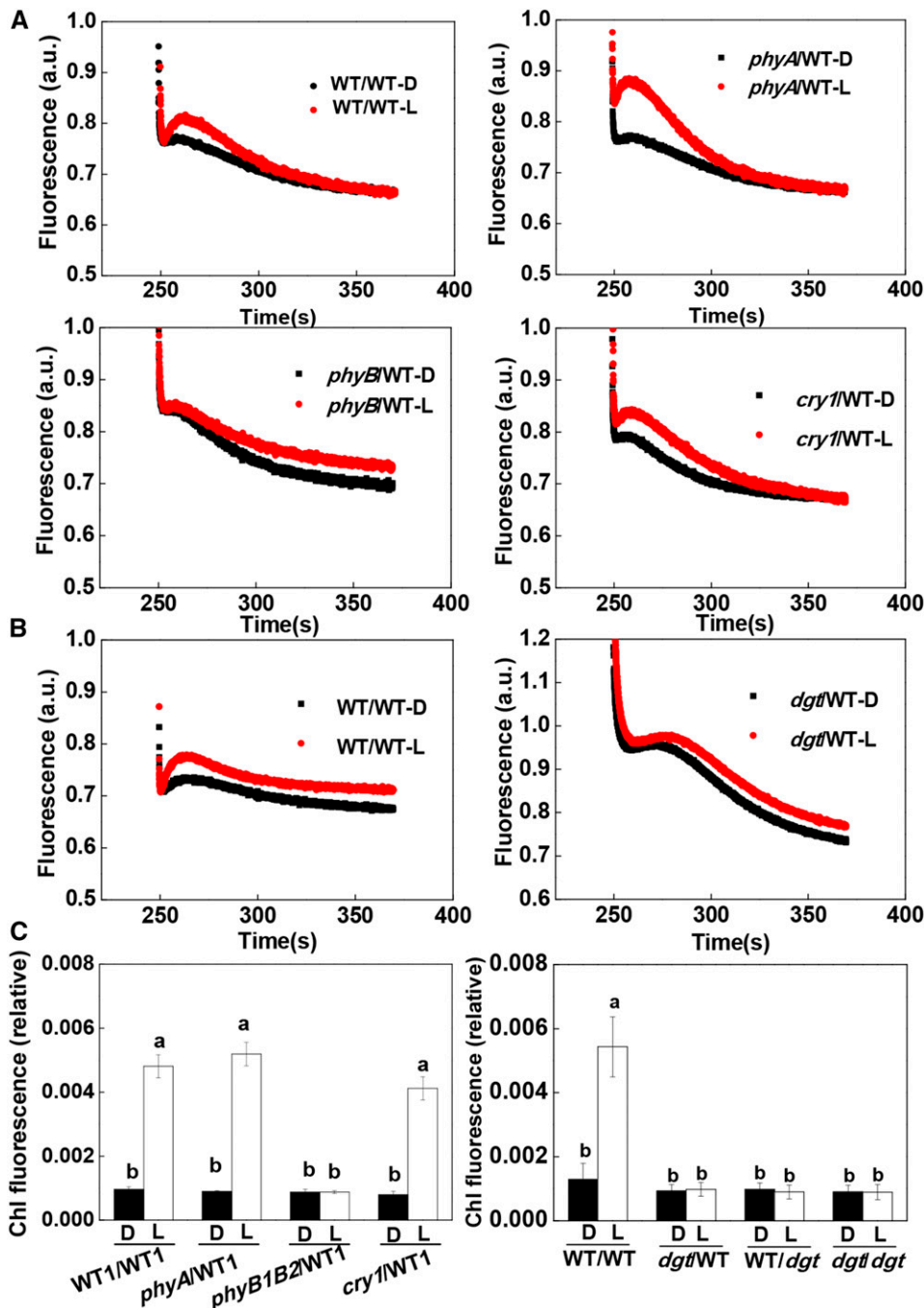


**Figure 6.** Effects of *phyA*, *phyB1B2*, and *cry1* as scions and *dgt* as scion or rootstock on the irradiance to the shoot apex-dependent changes in CEF. A, Typical traces chlorophyll *a* fluorescence quenching after 4 min of actinic illumination ( $250 \mu\text{mol m}^{-2} \text{s}^{-1}$ ) for grafted plants with different photoreceptor mutants as scions. B, Typical traces of chlorophyll *a* fluorescence quenching after 4 min of actinic illumination ( $250 \mu\text{mol m}^{-2} \text{s}^{-1}$ ) for plants with the *dgt* mutant as scion. C, Relative chlorophyll (Chl) fluorescence expressed as the ratio of the induction curve. Irradiance to the shoot apex (top lighting) was performed with WL (L) at  $300 \mu\text{mol m}^{-2} \text{s}^{-1}$  for 30 min. Plants without preillumination (dark [D]) were used as controls. During the illumination treatments, the other parts of the plant were kept in darkness. Values are means of four plants  $\pm$  SD. Different letters indicate significant differences at  $P < 0.05$  according to Tukey's test.

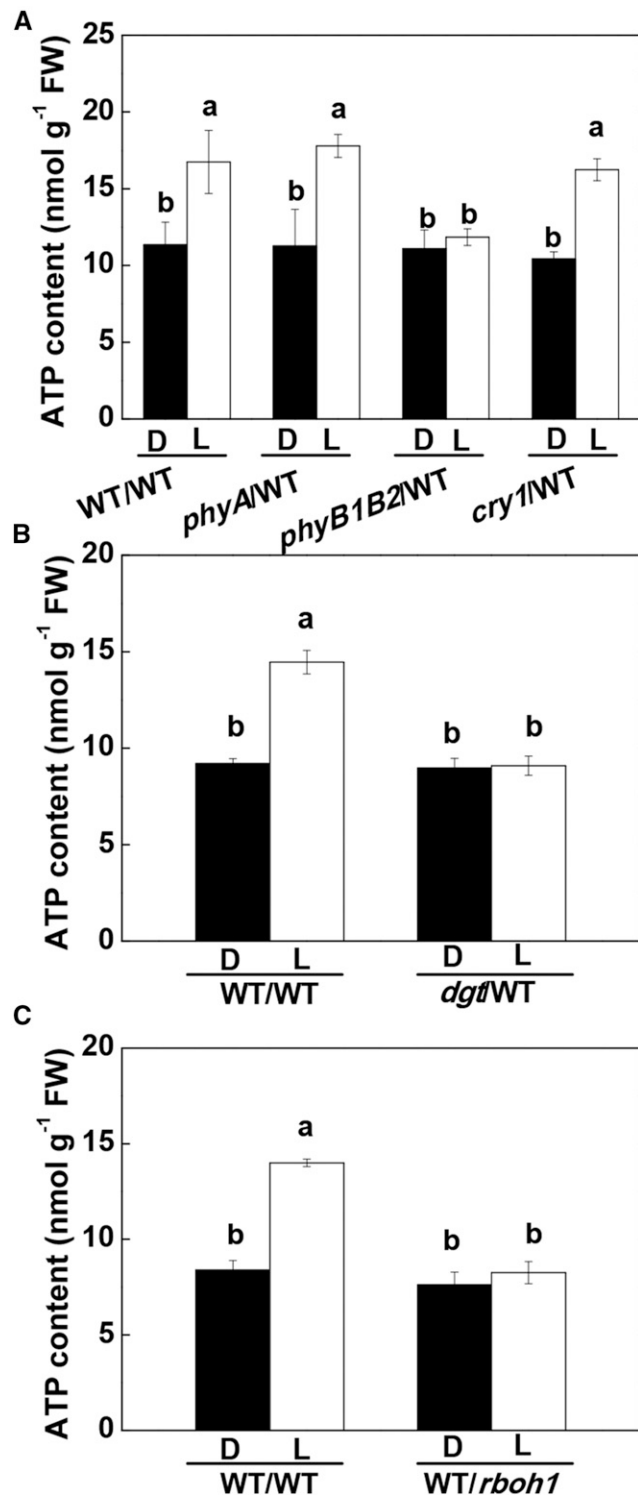


**Figure 7.** Influence of *phyA*, *phyB1B2*, and *cry1* (A) and *dgt* (B) as scions in grafted plants, and *RBOH1* suppression in the leaves of the rootstock (C), on the effects of irradiance to the apex on ATP accumulation in the fourth leaves. D, Dark control; L, WL (300  $\mu\text{mol m}^{-2} \text{s}^{-1}$ ) applied to the apex (top lighting) for 30 min. Samples were harvested after the fourth leaves were exposed to WL for 8 min with preillumination or not. During the illumination treatments, the other parts of the plant were kept in darkness. Values are means of four plants  $\pm$  sd.

### The Systemic Effects on Photosynthetic Induction Are Dependent on CEF in the Systemic Leaves

We next analyzed whether the increase in CEF is essential for the light-induced effects on photosynthetic induction in distal leaves. The *ORANGE RIPENING (ORR)* gene, which encodes an NAD(P)H dehydrogenase, was shown previously to be involved in the regulation of CEF in tomato (Nashilevitz et al., 2010). Virus-induced silencing of *ORR* (pTRV-*ORR*) resulted in a decrease in *ORR* transcript level of 68.7% compared with the empty vector plants (pTRV). Under high light, the pTRV-*ORR* plants showed very low CEF rates (Supplemental Fig. S10). Moreover, the pTRV-*ORR* plants showed no response to apical preillumination in term of the effects on the induction of  $\text{CO}_2$  assimilation and CEF (Fig. 8, A–D). While apical preillumination induced  $\text{H}_2\text{O}_2$  accumulation in the systemic leaves of both pTRV and pTRV-*ORR* plants (Fig. 8E), there was no increase in ATP levels in the pTRV-*ORR* plants (Fig. 8F).

### DISCUSSION

Rapid induction of photosynthesis in response to dark-to-light transitions and sharp increases in irradiance is critical to the survival of understory plants and gives a competitive advantage to plants within dense canopies. To date, studies on the induction of photosynthesis have been focused largely on responses in single leaves, with scant attention to the systemic integration of the leaf network within the plant. The results presented here demonstrate that phyB-mediated IAA synthesis in the shoot apex leads to systemic signaling and to  $\text{H}_2\text{O}_2$  accumulation in distal leaves. The subsequent increase in oxidation in the distal leaves activates CEF and ATP production, leading to a more rapid induction of  $\text{CO}_2$  assimilation (Fig. 9). This systemic response is likely linked to enhanced light use efficiency in a fluctuating light environment. Systemic signaling following the perception of light by the apex, which is the uppermost organ in the shoot, provides the distal leaves with a preemptive advantage in terms of the activation of photosynthesis and, hence, the ability to maximize carbon gain.

### The Apex-Induced Effects on the Induction of $\text{CO}_2$ Assimilation Are Phytochrome Dependent

Light drives photosynthetic electron transport as well as light quality and quantity affecting photosynthesis in different ways to optimize growth. The results presented here demonstrate that preillumination of the apex with WL and with R light results in a more rapid induction of photosynthesis in distal leaves (Fig. 1, A–D). This effect on photosynthetic induction is directional and was observed only after exposure of the apex to WL or R

Different letters indicate significant differences at  $P < 0.05$  according to Tukey's test. FW, Fresh weight.



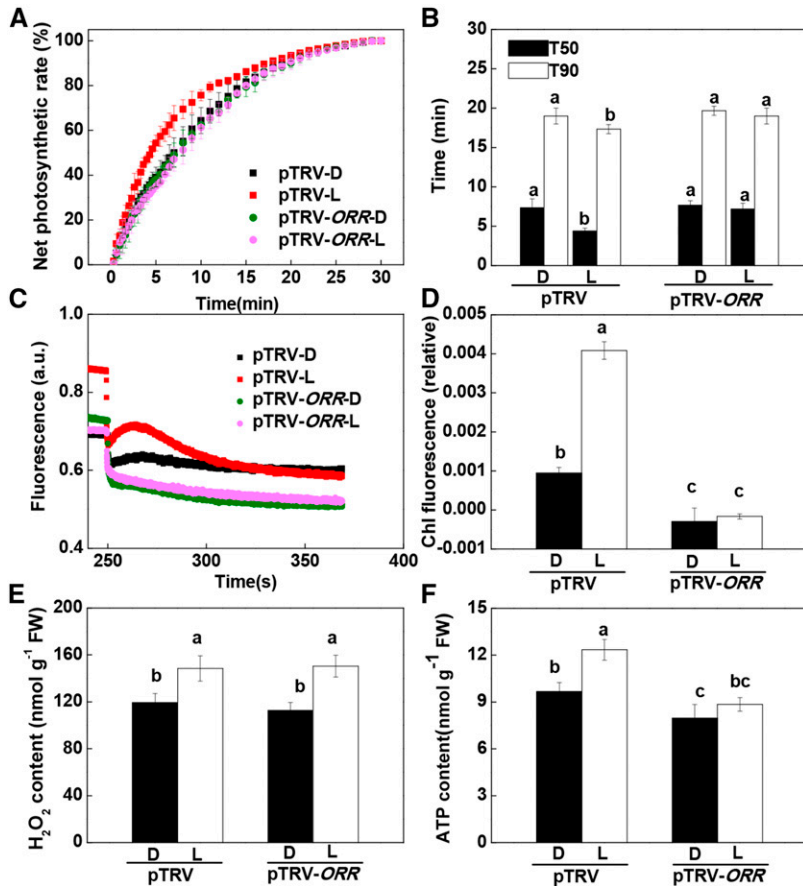


**Figure 8.** Requirement for *ORR* in systemic light signaling effects on the induction phase of photosynthesis in distal tomato leaves, including the time course of increases in net photosynthetic rate during photosynthetic induction, T50 or T90, CEF, H<sub>2</sub>O<sub>2</sub> accumulation, and ATP accumulation in the fourth leaves. A and B, Time course of increases in net photosynthetic rate during photosynthetic induction and T50 or T90 in fourth leaves. Net photosynthetic rates are expressed as percentages of the maximum net photosynthetic rate. C and D, Effect of *ORR* silencing on CEF in the fourth leaves during photosynthetic induction. a.u., Arbitrary unit. E, Effect of *ORR* on H<sub>2</sub>O<sub>2</sub> accumulation in the fourth leaves after preillumination of the apex with WL (L) at 300  $\mu\text{mol m}^{-2} \text{s}^{-1}$  for 30 min. F, Effect of *ORR* on ATP accumulation in the fourth leaves during photosynthetic induction. Samples were harvested after the fourth leaves were exposed to L for 8 min with preillumination. D, Dark control. During the illumination treatments, the other parts of the plant were kept in darkness. Values are means of four plants  $\pm$  sd. Different letters indicate significant differences at  $P < 0.05$  according to Tukey's test. Chl, Chlorophyll; FW, fresh weight.

light. This finding indicates that systemic signals originating from the young leaves at the apex, where cell division is rapid, are transduced to leaves in order to cause more rapid induction of photosynthesis. These observations are in agreement with an earlier observation that light-induced effects on photosynthesis are directional and that light perceived by mature leaves has little systemic effect on developing leaves in terms of the remodeling of photosynthesis (Murakami et al., 2014; Hou et al., 2015). The apex is likely to receive light signals earlier in the day than other parts of the plant. Thus, the transmission of light signals perceived at the apex to facilitate a more rapid photosynthetic induction in distal leaves probably evolved as a survival mechanism in understory plants in order to give a competitive advantage within dense canopies.

The rate of photosynthetic induction of distal leaves was modified by the quality of light perceived at the apex by photoreceptors present in the apex. R light and FR light had positive and negative effects, respectively, on the speed of photosynthetic induction (Fig. 1C). Interestingly, R light-induced photosynthetic induction could be abolished by FR light (Fig. 1E), suggesting that R and FR light-induced change in photosynthetic induction is a photochrome-dependent response. In agreement with this, grafting experiments using *phyA* and *phyB* mutants as the scion revealed that CO<sub>2</sub>

assimilation was induced more rapidly upon light perception by the apex in *phyA*/WT plants but not in the *phyB1B2*/WT combination (Fig. 1F; Supplemental Fig. S4). These findings suggest that *phyB* plays a key role in the systemic effects on the induction of photosynthesis. In agreement with these observations, *phyB* mutants show decreased CO<sub>2</sub> assimilation rates (Boccalandro et al., 2009), and conversely, overexpression of *PHYB* increased CO<sub>2</sub> assimilation rates compared with wild-type plants (Schittenhelm et al., 2004). Taken together, these results demonstrate that R light received by *phyB* at the shoot apex is the initial trigger for systemic signaling to the distal leaves.

#### Auxin Synthesized in the Apex Functions as a Systemic Signal Leading to Effects on the Induction of CO<sub>2</sub> Assimilation

Phytochrome signaling mediates many systemic responses in plants, including flowering time, tuberization, and nodule development, processes that are regulated by light-induced changes in phytohormone homeostasis (de Wit et al., 2016). Like PAT, the light-induced signaling pathway that influences photosynthetic induction is basipetal. Here, we provide multiple lines of evidence showing that auxin is required for the systemic effects on the induction of photosynthesis.

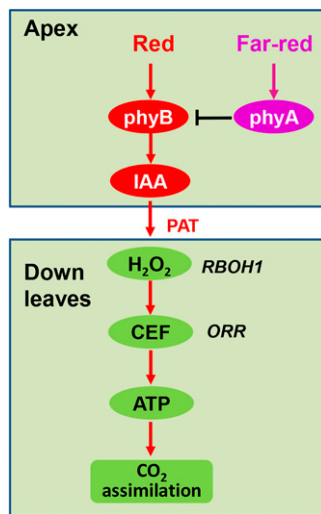


**Figure 9.** Working model depicting how light perception at the apex initiates an auxin- and redox-dependent systemic signaling pathway leading to enhanced rates of photosynthetic induction in distal leaves. In this model, R light perceived by phyB and FR light perceived by phyA function antagonistically to regulate IAA biosynthesis. As a result of light perception-driven PAT, IAA triggers systemic  $H_2O_2$  production in distal leaves, which is able to accelerate CEF around PSI, leading to increased ATP production. In this way, light perception by the apex can enhance photosynthetic  $CO_2$  assimilation and the resultant carbon gain in distal leaves.

First, WL and R light both induced an increase in *FZY* transcript levels in the apex, as well as IAA accumulation in the apex and an accumulation of *IAA15* transcripts, an auxin signaling marker in distal leaves (Fig. 2). Second, the transmission of light-induced signals from the apex that mediate systemic increases in the induction of  $CO_2$  assimilation was compromised in the wild-type leaves linked to a *phyB1B2* scion (Fig. 1F; Supplemental Fig. S4). Third, the application of IAA stimulated a more rapid induction of  $CO_2$  assimilation. Conversely, the application of an inhibitor of PAT compromised light-induced signal transmission to distal leaves (Fig. 3, A and B; Supplemental Fig. S6). Fourth, the transmission of light signals that enhance the induction of  $CO_2$  assimilation in systemic leaves was abolished when an auxin-resistant *dgt* mutant was used as the scion or rootstock (Fig. 3, C and D; Supplemental Fig. S7A). While we cannot rule out the potential involvement of light-induced carbohydrate accumulation and transport from the apex, the apex and the youngest leaves are defined as sink tissues that have a net import of carbohydrate to drive metabolism, growth, and development. These tissues are not generally considered to be source tissues, organs that export carbohydrate. Moreover, photosynthetic induction in distal leaves can be observed only after exposure to light intensities at PPFD levels higher than the light compensation point (Hou et al., 2015; Supplemental Fig. S2). We were unable to measure  $CO_2$  assimilation rates in apex leaves due to their small size. However,

$CO_2$  assimilation rates were very low in the developing leaves below the apex in the *phyB* plants, relative to the wild-type plants (Supplemental Fig. S11).

Soluble carbohydrates can regulate auxin biosynthesis via PHYTOCHROME-INTERACTING FACTOR (PIF) proteins, since PIFs negatively regulate phyB (Leivar et al., 2008; Sairanen et al., 2012). It is possible, therefore, that phyB functions as an integrator for light and sugar signaling in relation to auxin biosynthesis. To date, studies on the light regulation of auxin synthesis and PAT have produced contradictory results. For example, several studies have shown that exposure to low R/FR light ratios results in increased IAA accumulation and PAT in the hypocotyl (Tao et al., 2008; Keuskamp et al., 2010). However, such results have largely been obtained on very young *Arabidopsis* seedlings grown under conditions of minimal transpiration and photosynthesis, as occurs when plants are grown in closed petri dishes or on liquid medium often containing Suc, etc. (Tao et al., 2008; Keuskamp et al., 2010). Other studies have shown that low fluxes of R light enhance IAA synthesis and polar transport. The *phyB* mutant has decreased IAA accumulation in the stem in intact tomato plants (Liu et al., 2011). However, while plants grown under constant environmental conditions showed increased IAA accumulation during the night, plants grown in the field had increased IAA accumulation in the day (Lopez-Carbonell et al., 1992). Surprisingly, no studies have investigated the direct effects of light on auxin synthesis at the apex, even though auxin is thought to be synthesized mainly at the apex. Light- and phyB-mediated effects on IAA synthesis vary between organs and environments (Ballaré, 2014; Reddy and Finlayson, 2014). Plants may have developed these responses in auxin signaling as adaptation strategies to steep fluctuations in the light environment.

#### Auxin-Triggered $H_2O_2$ Production Acts as a Signal That Induces CEF and ATP Production in Systemic Leaves

Chloroplasts are a hub of redox control, which exerts a strong influence over gene expression, carbon assimilation, and starch synthesis (Fey et al., 2005; Pfannschmidt et al., 2009). Phytohormones such as brassinosteroids enhance  $CO_2$  assimilation rates in an RBOH-dependent manner in plants (Jiang et al., 2012). Moreover,  $H_2O_2$  activates CEF around PSI in order to increase  $CO_2$  assimilation (Strand et al., 2015). Auxin and brassinosteroids have overlapping functions in relation to the control of gene expression. Auxin also induces RBOH NADPH oxidase-dependent  $H_2O_2$  production (Ivanchenko et al., 2013; Peer et al., 2013). In this study, increased IAA accumulation and auxin signaling arising in the apex were shown to result in increased levels of *RBOH1* transcripts and in  $H_2O_2$  accumulation in systemic leaves, leading to increased CEF-dependent ATP production (Figs. 4–7). Crucially, blocking the auxin signal with a *dgt* scion or mutation of *RBOH1* genes in systemic leaves abolished the signal-induced CEF and ATP accumulation in the systemic

leaves (Figs. 5–7). Taken together, these results demonstrate that CEF can be regulated in distal leaves by the auxin-dependent  $H_2O_2$  production.

Noncyclic electron transport and CEF around PSI are used to generate a proton gradient across the thylakoid membrane, a process that is coupled with ATP production (Shikanai, 2007; Foyer et al., 2012). CEF around PSI in higher plants consists of at least two partially redundant pathways known as the ferredoxinquinone oxidoreductase- and NAD(P)H dehydrogenase (NDH)-dependent pathways (Miyake, 2010). NDH complex deficiency in *orr* mutant tomato plants was defective in CEF (Nashilevitz et al., 2010). Therefore,  $H_2O_2$ -induced CEF was not observed in mutants deficient in NDH. In our studies, suppression of NDH transcript using virus-induced gene silencing (VIGS) compromised the induction of CEF by systemic signals. These results show that the systemic effects on the induction of photosynthesis are linked to the regulation of NDH-dependent CEF (Fig. 8).

Switching between cyclic and noncyclic pathways provides flexibility in the ratios of ATP and NADPH produced by the electron transport chain. Therefore, the ratios of ATP to NADPH production can be adjusted to meet the needs of varying rates of Benson-Calvin cycle activity, photorespiration, and other metabolic pathways (Noctor and Foyer, 1999; Foyer et al., 2012). Thus, flexibility also allows rapid responses to fluctuations in the light environment (Foyer et al., 1992, 2012). In this regard, the systemic regulation of CEF may play a critical role in minimizing pseudocyclic electron flow and promoting the activation states of enzymes involved in  $CO_2$  fixation, such as Rubisco activase and Fru-1,6-bisphosphatase, which are modulated by the chloroplast redox status and ADP/ATP ratios, in the photosynthetic induction in response to irradiance.

The data presented here provide new insights into the regulation of photosynthesis. Evidence is presented showing that systemic regulation of the induction of photosynthesis in distal leaves is mediated by the perception of R light at the apex via a phyB-associated pathway that promotes IAA biosynthesis and PAT, as illustrated in Figure 9. As a result, *RBOH1*-dependent  $H_2O_2$  production in the systemic leaves induces CEF in the chloroplasts and associated ATP production. These systemic and local signaling processes accelerate the rate of induction of  $CO_2$  assimilation in systemic leaves. This study provides a mechanism by which plants can increase carbon gain in lower leaves in changing light environments via systemic regulation. Such mechanisms are likely to be very important in increasing light utilization efficiency in canopies, for example at dawn, or in understory leaves, where the light available in sunflecks must be used to maximize an advantage in driving carbon gain.

## MATERIALS AND METHODS

### Plant Material and Growth Conditions

Wild-type tomato (*Solanum lycopersicum* 'Ailsa Craig' and 'Moneymaker'), a cyclophilin A *dgt* mutant in the cv Ailsa Craig background, and *phyA*, *phyB1B2*,

and *cry1* mutants in the cv Moneymaker background were used unless stated otherwise. Seedlings were grown in pots with a mixture of three parts peat to one part vermiculite, receiving Hoagland nutrient solution. The growth conditions were as follows: 12-h photoperiod, temperature of 25°C/20°C (day/night), and PPFD of 600  $\mu\text{mol m}^{-2} \text{s}^{-1}$ .

To generate the *RBOH1* RNAi construct, a 318-bp specific DNA fragment of *SIRBOH1* was PCR amplified with the specific primers *SIRBOH1-F* (5'-GGCCatttaaatggatccCGTTCAGCTCTCATTACC-3') and *SIRBOH1-R* (5'-TTggcgcgcctctagaCCGAAGATAGATGTGTGT-3'), which had been tailed with *Bam*HI/*Xba*I and *Swa*I/*Asc*I restriction sites at the 5' end, respectively. Then, the amplified products were digested with *Bam*HI/*Xba*I and *Swa*I/*Asc*I and ligated into the pFGC5941 vector at the *Bam*HI/*Xba*I restriction sites in the sense orientation and at the *Swa*I/*Asc*I restriction sites in the antisense orientation. The resulting plasmid was transformed into *Agrobacterium tumefaciens* strain EHA105 and into tomato cotyledons of cv Ailsa Craig as described by Fillatti et al. (1987). Transgenic plants were identified for resistance to Basta and then by quantitative reverse transcription (qRT)-PCR analysis.

To determine the role of cyclic electron flux in preillumination-induced  $CO_2$  assimilation, we used VIGS to suppress the transcript of *ORR* (Nashilevitz et al., 2010) with the tobacco rattle virus (TRV)-based vectors pTRV1/2 (Liu et al., 2002). The *ORR* cDNA fragment was PCR amplified using the forward primer 5'-CGgaattcGATCCCGAAACCTTTGCTT-3' and the reverse primer 5'-CCGctcgagTCACATTGTAATTGAACCCA-3'. The amplified *ORR* fragment was digested with *Eco*RI and *Xho*I and ligated into the corresponding sites of the pTRV2 vector. Empty pTRV2 vector was used as a control. All constructs were confirmed by sequencing and subsequently transformed into *A. tumefaciens* strain GV3101. VIGS was performed by infiltration into the fully expanded cotyledons of 15-d-old tomato seedlings with *A. tumefaciens* harboring a mixture of pTRV1 and pTRV2 target genes in a 1:1 ratio. Plants were grown at 21°C in a growth chamber with a 12-h daylength for 30 d until control pTRV-*PDS* plants (silencing of the gene encoding phytoene desaturase) showed strong bleaching (Ekengren et al., 2003). qRT-PCR was performed to determine the gene silencing efficiency (Livak and Schmittgen, 2001).

To determine the role of photoreceptors in photosynthetic induction, shoots of wild type, *phyA*, *phyB1B2*, and *cry1* plants with two developing leaves at 3 to 4 cm in length were grafted onto the fourth leaf stem of wild-type plants, resulting in four groups of seedlings designated as WT/WT, *phyA*/WT, *phyB1B2*/WT, and *cry1*/WT, according to the scions. In the same way, we grafted shoots with two leaves of *dgt* mutant plants, which is auxin resistant, onto the stem of wild-type plants (*dgt*/WT), wild-type shoots onto the stem of *dgt* plants (WT/*dgt*) or onto that of *RBOH1* RNAi plants (WT/*rbol1*), and shoots of *RBOH1* RNAi plants onto *RBOH1* RNAi plants (*rbol1*/*rbol1*). The grafted plants were transferred to growth chambers with the following environmental conditions: 12-h photoperiod, temperature of 25°C/20°C (day/night), and PPFD of 600  $\mu\text{mol m}^{-2} \text{s}^{-1}$ .

### Experimental Design and Treatments

Leaves on a plant were marked from number 1 to number 6 from cotyledons. Six independent experiments were carried out. In experiment 1, the first to third leaves, the fifth and sixth leaves, and the apex were illuminated with WL (Philips) at 50, 150, and 300  $\mu\text{mol m}^{-2} \text{s}^{-1}$  for 30 min before the photosynthetic induction of the fourth leaf was measured (Supplemental Fig. S1). In experiment 2, the apex of wild-type plants at the six-leaf stage was illuminated with R light (660 nm) or FR light (735 nm) at 300  $\mu\text{mol m}^{-2} \text{s}^{-1}$  for 30 min or light with an R/FR light ratio at 2:1, 1:1, and 1:2, in which R light intensity was kept at 300  $\mu\text{mol m}^{-2} \text{s}^{-1}$ . Meanwhile, a reciprocal R/FR light pulse at 5-min intervals, which lasted 60 min with six cycles, was applied to the apex to test the reversibility of the positive effect of R light on photosynthetic induction. Monospectrum light was supplied with a light-emitting diode source (Philips). In other experiments, the apex of WT/WT, *phyA*/WT, *phyB1B2*/WT, and *cry1*/WT (experiment 3), *dgt*/WT and WT/*dgt* (experiment 4), WT/*rbol1* and *rbol1*/*rbol1* (experiment 5), and pTRV and pTRV-*ORR* (experiment 6) plants at the six-leaf stage was preilluminated with WL at 300  $\mu\text{mol m}^{-2} \text{s}^{-1}$  for 30 min before the photosynthetic induction of the fourth leaf was measured. To study the role of IAA in photosynthetic induction, IAA at 10  $\mu\text{M}$  and NPA at 10  $\mu\text{M}$  were applied on the apex 30 min before gas exchange in the fourth leaf was determined. In all cases, plants without preillumination of the apex (dark) were used as controls.

### Gas Exchange and Chlorophyll Fluorescence

Gas-exchange measurements were performed using the LI-6400 Portable Photosynthesis System (LI-COR). The  $CO_2$  concentration (400  $\mu\text{mol mol}^{-1}$ ), air

humidity (60%), PPFD ( $1,500 \mu\text{mol m}^{-2} \text{s}^{-1}$ ), and leaf temperature ( $25^\circ\text{C}$ ) were controlled by an automatic control device of the instrument. The photosynthetic rate was recorded every 20 s. Four plants were used in each measurement.

Chlorophyll fluorescence was measured using a Dual-PAM 100 chlorophyll fluorescence analyzer (Heinz Walz) as described by Gotoh et al. (2010). For the determination of chlorophyll fluorescence, plants were adapted in the dark for 30 min prior to measurement. After 4 min, the actinic light ( $250 \mu\text{mol m}^{-2} \text{s}^{-1}$ ) was turned off and fluorescence yield changes were recorded continuously (Yang et al., 2007). Four plants were used for each replicate. Relative chlorophyll fluorescence, expressed as the rake ratio of the induction curve, was calculated from the one-time regression equation  $y = a + bx$ , where  $y$ ,  $a$ , and  $x$  are the fluorescence yield, the rake ratio of the induction curve, and the duration time, respectively, during the fluorescence rise.

## Measurement of IAA Levels

IAA extraction and quantification were performed using previously reported procedures with minor modifications (Durgbanshi et al., 2005; Wu et al., 2007; Boelaert et al., 2013). Briefly, 100 mg of frozen leaf material was homogenized in 1 mL of ethyl acetate that had been spiked with D<sub>5</sub>-IAA (C/D/N Isotopes) as an internal standard at a final concentration of  $100 \text{ ng mL}^{-1}$ . Tubes were centrifuged at  $18,000g$  for 10 min at  $4^\circ\text{C}$ . The pellet was reextracted with 1 mL of ethyl acetate. Both supernatants were evaporated to dryness under N<sub>2</sub>. The residue was resuspended in 0.5 mL of 70% (v/v) methanol and centrifuged, and the supernatants were then analyzed in a liquid chromatography-tandem mass spectrometry system (Varian 320-MS LC/MS; Agilent Technologies). The parent ions, daughter ions, and collision energies used in these analyses are listed in Supplemental Table S1.

## H<sub>2</sub>O<sub>2</sub> Quantification, Histochemical Analysis, and Cytochemical Detection

H<sub>2</sub>O<sub>2</sub> was extracted from leaf tissue and measured as described in our earlier study (Xia et al., 2009). H<sub>2</sub>O<sub>2</sub> also was visualized at the subcellular level using CeCl<sub>3</sub> for localization, as described previously (Zhou et al., 2012). The sections were examined using a transmission electron microscope (H7650; Hitachi) at an accelerating voltage of 75 kV to detect the electron-dense CeCl<sub>3</sub> deposits that were formed in the presence of H<sub>2</sub>O<sub>2</sub>.

## qRT-PCR Analysis

Total RNA was extracted from tomato leaves using the RNeasy Pure Plant Kit (Qiagen) according to the supplier's recommendation. Residual DNA was removed with the RNase Mini Kit (Qiagen). One microgram of total RNA was reverse transcribed using the ReverTra Ace qPCR RT Kit (Toyobo) following the supplier's recommendation. On the basis of EST sequences, the gene-specific primers are shown in Supplemental Table S2 and used for amplification. qRT-PCR was performed using the LightCycler 480 real-time PCR machine (Roche). The PCR was run for  $95^\circ\text{C}$  for 3 min, followed by 40 cycles of 30 s at  $95^\circ\text{C}$ , 30 s at  $58^\circ\text{C}$ , and 1 min at  $72^\circ\text{C}$ . The tomato *ACTIN* gene was used as an internal control. Relative gene expression was calculated as described previously (Livak and Schmittgen, 2001).

## Determination of ATP Content

To determine ATP content in leaves, 0.1-g leaf samples were immediately placed in tubes containing 2 mL of Tris-HCl (pH 7.8). The tubes with samples were then kept for 10 min at  $100^\circ\text{C}$  in a boiling water bath for ATP extraction. One hundred microliters of ATP extraction solution was used for analysis after sample cooling at room temperature. The procedure was performed following the instructions in the ATPlite 1step Assay System (Perkin-Elmer).

## Supplemental Data

The following supplemental materials are available.

**Supplemental Figure S1.** Sketch map of the plant materials and experiment design.

**Supplemental Figure S2.** Effects of preillumination at different WL intensities on the induction of photosynthesis in the systemic leaves.

**Supplemental Figure S3.** Effects of preillumination on the induction of photosynthesis in plants with *cry1* as scion.

**Supplemental Figure S4.** Influence of systemic light signaling on the time required to reach T50 or T90 in photosynthetic induction.

**Supplemental Figure S5.** Relative transcript of *PIN1* in the fourth leaf as influenced by preillumination.

**Supplemental Figure S6.** Effects of the application of NPA on the induction of photosynthesis.

**Supplemental Figure S7.** Effects of preillumination on the induction of photosynthesis and CEF in the fourth leaf in grafting plants with *dgt* as rootstock.

**Supplemental Figure S8.** Relative transcript of *RBOH1* in the scion leaves and rootstock leaves in grafted plants used for the experiment ( $n = 12$ ).

**Supplemental Figure S9.** Time course of the net photosynthetic rate and CEF in the fourth leaf as influenced by the suppressed transcript of *RBOH1* in grafted plants.

**Supplemental Figure S10.** Cyclic electron flux and relative transcript of *ORR* in VIGS plants used for the experiment.

**Supplemental Figure S11.** CO<sub>2</sub> assimilation rate for wild-type and phyB plants.

**Supplemental Table S1.** Parameters used for the detection of IAA and related compounds by liquid chromatography-tandem mass spectrometry.

**Supplemental Table S2.** Primer sequences used for qRT-PCR analysis.

## ACKNOWLEDGMENTS

We thank the Tomato Genetics Resource Center at the University of California, Davis, for tomato phytochrome mutants, Dr. M.G. Ivanchenko (Oregon State University) for providing *dgt* seeds, and Xiaodan Wu (Analysis Center of Agrobiological and Environmental Sciences, Institute of Agrobiological and Environmental Sciences, Zhejiang University) for assistance with phytohormone analysis.

Received August 1, 2016; accepted August 19, 2016; published August 22, 2016.

## LITERATURE CITED

- Allen JF (2003) Cyclic, pseudocyclic and noncyclic photophosphorylation: new links in the chain. *Trends Plant Sci* **8**: 15–19
- Araya T, Noguchi K, Terashima I (2008) Manipulation of light and CO<sub>2</sub> environments of the primary leaves of bean (*Phaseolus vulgaris* L.) affects photosynthesis in both the primary and the first trifoliate leaves: involvement of systemic regulation. *Plant Cell Environ* **31**: 50–61
- Bai KD, Liao DB, Jiang DB, Cao KF (2008) Photosynthetic induction in leaves of co-occurring *Fagus lucida* and *Castanopsis lamontii* saplings grown in contrasting light environments. *Trees (Berl)* **22**: 449–462
- Ballaré CL (2014) Light regulation of plant defense. *Annu Rev Plant Biol* **65**: 335–363
- Bidwell RG, Turner WB (1966) Effect of growth regulators on CO<sub>2</sub> assimilation in leaves, and its correlation with the bud break response in photosynthesis. *Plant Physiol* **41**: 267–270
- Boccalandro HE, Rugnone ML, Moreno JE, Ploschuk EL, Serna L, Yanovsky MJ, Casal JJ (2009) Phytochrome B enhances photosynthesis at the expense of water-use efficiency in Arabidopsis. *Plant Physiol* **150**: 1083–1092
- Boelaert J, Lynen F, Glorieux G, Eloit S, Van Landschoot M, Waterlooos MA, Sandra P, Vanholder R (2013) A novel UPLC-MS-MS method for simultaneous determination of seven uremic retention toxins with cardiovascular relevance in chronic kidney disease patients. *Anal Bioanal Chem* **405**: 1937–1947
- Casson SA, Hetherington AM (2014) Phytochrome B is required for light-mediated systemic control of stomatal development. *Curr Biol* **24**: 1216–1221
- Coupe SA, Palmer BG, Lake JA, Overy SA, Oxborough K, Woodward FI, Gray JE, Quick WP (2006) Systemic signalling of environmental cues in Arabidopsis leaves. *J Exp Bot* **57**: 329–341
- Deng W, Yang Y, Ren Z, Audran-Delalande C, Mila I, Wang X, Song H, Hu Y, Bouzayen M, Li Z (2012) The tomato *SIIAA15* is involved in

- trichome formation and axillary shoot development. *New Phytol* **194**: 379–390
- de Wit M, Galvão VC, Fankhauser C (2016) Light-mediated hormonal regulation of plant growth and development. *Annu Rev Plant Biol* **67**: 513–537
- Durgbanshi A, Arbona V, Pozo O, Miersch O, Sancho JV, Gómez-Cadenas A (2005) Simultaneous determination of multiple phytohormones in plant extracts by liquid chromatography-electrospray tandem mass spectrometry. *J Agric Food Chem* **53**: 8437–8442
- Ekengren SK, Liu Y, Schiff M, Dinesh-Kumar SP, Martin GB (2003) Two MAPK cascades, NPR1, and TGA transcription factors play a role in Pto-mediated disease resistance in tomato. *Plant J* **36**: 905–917
- Fey V, Wagner R, Bräutigam K, Pfannschmidt T (2005) Photosynthetic redox control of nuclear gene expression. *J Exp Bot* **56**: 1491–1498
- Fillatti JAJ, Kiser J, Rose R, Comai L (1987) Efficient transfer of a glyphosate tolerance gene into tomato using a binary *Agrobacterium tumefaciens* vector. *Nat Biotechnol* **5**: 726–730
- Foyer CH, Lelandais M, Harbinson J (1992) Control of the quantum efficiencies of photosystems I and II, electron flow, and enzyme activation following dark-to-light transitions in pea leaves: relationship between NADP/NADPH ratios and NADP-malate dehydrogenase activation state. *Plant Physiol* **99**: 979–986
- Foyer CH, Neukermans J, Queval G, Noctor G, Harbinson J (2012) Photosynthetic control of electron transport and the regulation of gene expression. *J Exp Bot* **63**: 1637–1661
- Fu ZQ, Dong X (2013) Systemic acquired resistance: turning local infection into global defense. *Annu Rev Plant Biol* **64**: 839–863
- Geldner N, Friml J, Stierhof YD, Jürgens G, Palme K (2001) Auxin transport inhibitors block PIN1 cycling and vesicle trafficking. *Nature* **413**: 425–428
- Gotoh E, Kobayashi Y, Tsuyama M (2010) The post-illumination chlorophyll fluorescence transient indicates the RuBP regeneration limitation of photosynthesis in low light in Arabidopsis. *FEBS Lett* **584**: 3061–3064
- Halliday KJ, Martínez-García JF, Josse EM (2009) Integration of light and auxin signaling. *Cold Spring Harb Perspect Biol* **1**: a001586
- Hauser BA, Cordonnier-Pratt MM, Daniel-Vedele F, Pratt LH (1995) The phytochrome gene family in tomato includes a novel subfamily. *Plant Mol Biol* **29**: 1143–1155
- Hayat Q, Hayat S, Ali B, Aqil A (2009) Auxin analogues and nitrogen metabolism, photosynthesis, and yield of chickpea. *J Plant Nutr* **32**: 1469–1485
- Hou F, Jin LQ, Zhang ZS, Gao HY (2015) Systemic signalling in photosynthetic induction of *Rumex* K-1 (*Rumex patientia* × *Rumex tianschaisicus*) leaves. *Plant Cell Environ* **38**: 685–692
- Ivanchenko MG, den Os D, Monshausen GB, Dubrovsky JG, Bednárová A, Krishnan N (2013) Auxin increases the hydrogen peroxide (H<sub>2</sub>O<sub>2</sub>) concentration in tomato (*Solanum lycopersicum*) root tips while inhibiting root growth. *Ann Bot (Lond)* **112**: 1107–1116
- Ivanchenko MG, Zhu J, Wang B, Medvecká E, Du Y, Azzarello E, Mancuso S, Megraw M, Filichkin S, Dubrovsky JG, et al (2015) The cyclophilin A DIAGEOTROPICA gene affects auxin transport in both root and shoot to control lateral root formation. *Development* **142**: 712–721
- Jiang YP, Cheng F, Zhou YH, Xia XJ, Mao WH, Shi K, Chen Z, Yu JQ (2012) Cellular glutathione redox homeostasis plays an important role in the brassinosteroid-induced increase in CO<sub>2</sub> assimilation in *Cucumis sativus*. *New Phytol* **194**: 932–943
- Jiao Y, Lau OS, Deng XW (2007) Light-regulated transcriptional networks in higher plants. *Nat Rev Genet* **8**: 217–230
- Joët T, Cournac L, Peltier G, Havaux M (2002) Cyclic electron flow around photosystem I in C<sub>3</sub> plants: in vivo control by the redox state of chloroplasts and involvement of the NADH-dehydrogenase complex. *Plant Physiol* **128**: 760–769
- Joliot P, Joliot A (2002) Cyclic electron transfer in plant leaf. *Proc Natl Acad Sci USA* **99**: 10209–10214
- Keuskamp DH, Pollmann S, Voesenek LACJ, Peeters AJM, Pierik R (2010) Auxin transport through PIN-FORMED 3 (PIN3) controls shade avoidance and fitness during competition. *Proc Natl Acad Sci USA* **107**: 22740–22744
- Lake JA, Woodward FI, Quick WP (2002) Long-distance CO<sub>2</sub> signalling in plants. *J Exp Bot* **53**: 183–193
- Leakey ADB, Press MC, Scholes JD (2003) Patterns of dynamic irradiance affect the photosynthetic capacity and growth of dipterocarp tree seedlings. *Oecologia* **135**: 184–193
- Leakey ADB, Scholes JD, Press MC (2005) Physiological and ecological significance of sunflecks for dipterocarp seedlings. *J Exp Bot* **56**: 469–482
- Leivar P, Monte E, Al-Sady B, Carle C, Storer A, Alonso JM, Ecker JR, Quail PH (2008) The *Arabidopsis* phytochrome-interacting factor PIF7, together with PIF3 and PIF4, regulates responses to prolonged red light by modulating phyB levels. *Plant Cell* **20**: 337–352
- Liu X, Cohen JD, Gardner G (2011) Low-fluence red light increases the transport and biosynthesis of auxin. *Plant Physiol* **157**: 891–904
- Liu Y, Schiff M, Marathe R, Dinesh-Kumar SP (2002) Tobacco *Rar1*, *EDS1* and *NPR1/NIMI* like genes are required for N-mediated resistance to tobacco mosaic virus. *Plant J* **30**: 415–429
- Livak KJ, Schmittgen TD (2001) Analysis of relative gene expression data using real-time quantitative PCR and the 2<sup>(-ΔΔCT)</sup> method. *Methods* **25**: 402–408
- Ljung K, Bhalarao RP, Sandberg G (2001) Sites and homeostatic control of auxin biosynthesis in Arabidopsis during vegetative growth. *Plant J* **28**: 465–474
- Lopez-Carbonell M, Alegre L, Prinsen E, Onckelen HV (1992) Diurnal fluctuations of endogenous IAA content in aralia leaves. *Biol Plant* **34**: 223–227
- Mittler R, Blumwald E (2015) The roles of ROS and ABA in systemic acquired acclimation. *Plant Cell* **27**: 64–70
- Miyake C (2010) Alternative electron flows (water-water cycle and cyclic electron flow around PSI) in photosynthesis: molecular mechanisms and physiological functions. *Plant Cell Physiol* **51**: 1951–1963
- Montgomery RA, Givnish TJ (2008) Adaptive radiation of photosynthetic physiology in the Hawaiian lobeliads: dynamic photosynthetic responses. *Oecologia* **155**: 455–467
- Murakami K, Matsuda R, Fujiwara K (2014) Light-induced systemic regulation of photosynthesis in primary and trifoliate leaves of *Phaseolus vulgaris*: effects of photosynthetic photon flux density (PPFD) versus spectrum. *Plant Biol (Stuttg)* **16**: 16–21
- Nashilevitz S, Melamed-Bessudo C, Izkovitch Y, Rogachev I, Osorio S, Itkin M, Adato A, Pankratov I, Hirschberg J, Fernie AR, et al (2010) An orange ripening mutant links plastid NAD(P)H dehydrogenase complex activity to central and specialized metabolism during tomato fruit maturation. *Plant Cell* **22**: 1977–1997
- Noctor G, Foyer CH (1999) A re-evaluation of the ATP:NADPH budget during C<sub>3</sub> photosynthesis: a contribution from nitrate assimilation and its associated respiratory activity? *J Exp Bot* **49**: 1895–1908
- Pearcy RW, Seemann JR (1990) Photosynthetic induction state of leaves in a soybean canopy in relation to light regulation of ribulose-1,5-bisphosphate carboxylase and stomatal conductance. *Plant Physiol* **94**: 628–633
- Peer WA, Cheng Y, Murphy AS (2013) Evidence of oxidative attenuation of auxin signalling. *J Exp Bot* **64**: 2629–2639
- Peng Q, Wang H, Tong J, Kabir MH, Huang Z, Xiao L (2013) Effects of indole-3-acetic acid and auxin transport inhibitor on auxin distribution and development of peanut at pegging stage. *Sci Hortic (Amsterdam)* **162**: 76–81
- Pfannschmidt T, Bräutigam K, Wagner R, Dietzel L, Schröter Y, Steiner S, Nykytenko A (2009) Potential regulation of gene expression in photosynthetic cells by redox and energy state: approaches towards better understanding. *Ann Bot (Lond)* **103**: 599–607
- Pieterse CMJ, Dicke M (2007) Plant interactions with microbes and insects: from molecular mechanisms to ecology. *Trends Plant Sci* **12**: 564–569
- Reddy SK, Finlayson SA (2014) Phytochrome B promotes branching in Arabidopsis by suppressing auxin signaling. *Plant Physiol* **164**: 1542–1550
- Sairanen I, Novak O, Pencik A, Ikeda Y, Jones B, Sandberg G, Ljung K (2012) Soluble carbohydrates regulate auxin biosynthesis via PIF proteins in *Arabidopsis*. *Plant Cell* **24**: 4907–4916
- Schittenhelm S, Menge-Hartmann U, Oldenburg E (2004) Photosynthesis, carbohydrate metabolism, and yield of phytochrome-B-overexpressing potatoes under different light regimes. *Crop Sci* **44**: 131–143
- Shikanai T (2007) Cyclic electron transport around photosystem I: genetic approaches. *Annu Rev Plant Biol* **58**: 199–217
- Strand DD, Livingston AK, Satoh-Cruz M, Froehlich JE, Maurino VG, Kramer DM (2015) Activation of cyclic electron flow by hydrogen peroxide in vivo. *Proc Natl Acad Sci USA* **112**: 5539–5544
- Tao Y, Ferrer JL, Ljung K, Pojer F, Hong F, Long JA, Li L, Moreno JE, Bowman ME, Ivans LJ, et al (2008) Rapid synthesis of auxin via a new tryptophan-dependent pathway is required for shade avoidance in plants. *Cell* **133**: 164–176
- Thorpe MR, Ferrieri AP, Herth MM, Ferrieri RA (2007) <sup>14</sup>C-imaging: methyl jasmonate moves in both phloem and xylem, promotes transport of jasmonate, and of photoassimilate even after proton transport is decoupled. *Planta* **226**: 541–551

- Tivendale ND, Davies NW, Molesworth PP, Davidson SE, Smith JA, Lowe EK, Reid JB, Ross JJ** (2010) Reassessing the role of *N*-hydroxytryptamine in auxin biosynthesis. *Plant Physiol* **154**: 1957–1965
- Turgeon R, Wolf S** (2009) Phloem transport: cellular pathways and molecular trafficking. *Annu Rev Plant Biol* **60**: 207–221
- Walker DA** (1973) Photosynthetic induction phenomena and light activation of ribulose diphosphate carboxylase. *New Phytol* **72**: 209–235
- Wang F, Guo Z, Li H, Wang M, Onac E, Zhou J, Xia X, Shi K, Yu J, Zhou Y** (2016) Phytochrome A and B function antagonistically to regulate cold tolerance via abscisic acid-dependent jasmonate signaling. *Plant Physiol* **170**: 459–471
- Weller JL, Schreuder ME, Smith H, Koornneef M, Kendrick RE** (2000) Physiological interactions of phytochromes A, B1 and B2 in the control of development in tomato. *Plant J* **24**: 345–356
- Wu J, Hettenhausen C, Meldau S, Baldwin IT** (2007) Herbivory rapidly activates MAPK signaling in attacked and unattacked leaf regions but not between leaves of *Nicotiana attenuata*. *Plant Cell* **19**: 1096–1122
- Xia XJ, Wang YJ, Zhou YH, Tao Y, Mao WH, Shi K, Asami T, Chen Z, Yu JQ** (2009) Reactive oxygen species are involved in brassinosteroid-induced stress tolerance in cucumber. *Plant Physiol* **150**: 801–814
- Xia XJ, Zhou YH, Shi K, Zhou J, Foyer CH, Yu JQ** (2015) Interplay between reactive oxygen species and hormones in the control of plant development and stress tolerance. *J Exp Bot* **66**: 2839–2856
- Yamori W, Shikanai T** (2016) Physiological functions of cyclic electron transport around photosystem I in sustaining photosynthesis and plant growth. *Annu Rev Plant Biol* **67**: 81–106
- Yamori W, Shikanai T, Makino A** (2015) Photosystem I cyclic electron flow via chloroplast NADH dehydrogenase-like complex performs a physiological role for photosynthesis at low light. *Sci Rep* **5**: 13908
- Yang Y, Yan CQ, Cao BH, Xu HX, Chen JP, Jiang DA** (2007) Some photosynthetic responses to salinity resistance are transferred into the somatic hybrid descendants from the wild soybean *Glycine cyrtoloba* ACC547. *Physiol Plant* **129**: 658–669
- Zhou J, Wang J, Shi K, Xia XJ, Zhou YH, Yu JQ** (2012) Hydrogen peroxide is involved in the cold acclimation-induced chilling tolerance of tomato plants. *Plant Physiol Biochem* **60**: 141–149
- Zimmermann MR, Maischak H, Mithöfer A, Boland W, Felle HH** (2009) System potentials, a novel electrical long-distance apoplastic signal in plants, induced by wounding. *Plant Physiol* **149**: 1593–1600